2
Road vehicle modeling

2.1
Simple handling model

Originally named as the "Bicycle Model", this model was established by Riekert and Schunck in 1940. Throughout this thesis, the "Bicycle Model" is refereed as the simple handling model (SHM). This model is a simplification of a four-wheeled road vehicle which considers the Ackermann steering geometry. It assumes a centered substitute wheel at each axle. Furthermore, these wheels represent the characteristics of the wheel/axle suspensions and tires of the related axle. Figure 10 displays a four-wheeled car and its simplified two-wheeled model during a steady state-cornering at low speeds.

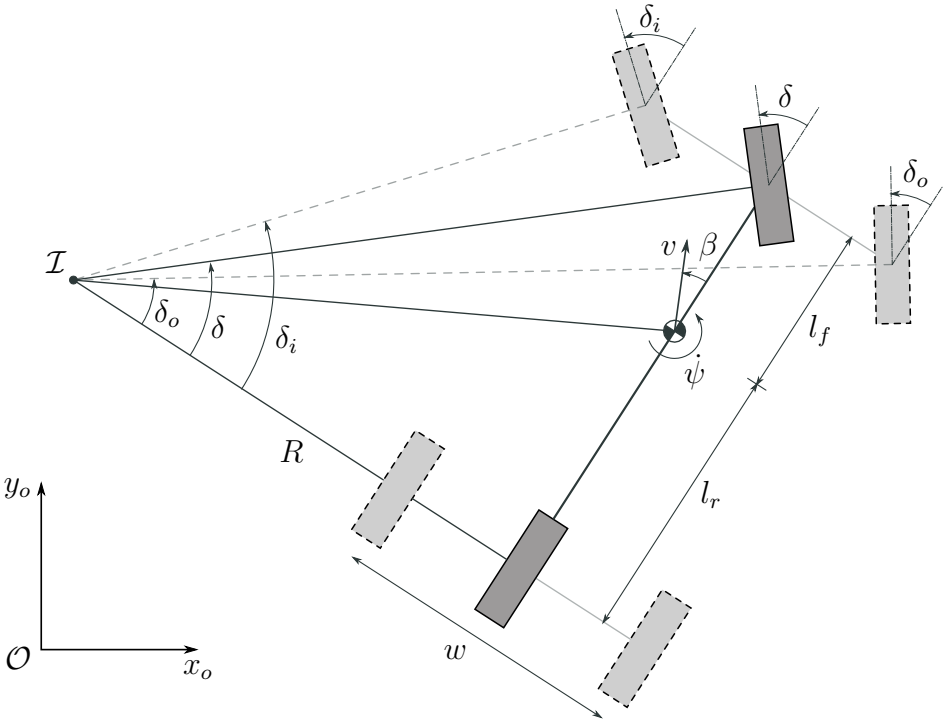

Figure 10: Simple handling model (SHM) during a steady-state cornering at low speeds.

During a steady-state cornering at low speeds, the centrifugal force can be neglected. Therefore, the steering wheel angles at the inner (δ_i) and outer (δ_o) wheels can be defined as

$$\tan(\delta_i) = \frac{l}{R - w/2} \quad \text{and} \quad \tan(\delta_o) = \frac{l}{R + w/2}, \tag{2-1}$$

where R is the radius of curvature of the rear substitute wheel around the instantaneous center of rotation ($\mathcal{I}$); $l = l_f + l_r$ is also know as the vehicle's wheel-base and w its track-width. Then, rearranging the Equation (2-1), it is possible to define the Ackermann steering geometry via

$$\cot(\delta_o) - \cot(\delta_i) = \frac{w}{l}. \tag{2-2}$$

This Ackermann condition is fulfilled only for small speeds. However, in most cases, cars will perform a curve at considerable speeds. Therefore, the deviation $\Delta\delta = \delta_o^a - \delta_o^A$, obtained by the difference between the actual steering wheel angle δ_o^a and the one computed using the Equation (2-2), i.e. δ_o^A, is used as a quality indicator of the steering system of commercial vehicles. Finally, it is also possible to calculate the steering wheel angle of the SHM (δ) via

$$\tan(\delta) = \frac{l}{R} \quad \text{or} \quad \cot(\delta) = \frac{\cot(\delta_o) + \cot(\delta_i)}{2}. \tag{2-3}$$

At high vehicle's speeds, the position of $\mathcal{I}$ will change depending on the road and vehicle conditions as shown in Figure 11. Furthermore, it is necessary to consider the lateral acceleration and therefore, the centrifugal force at the center of gravity. Then, an earth-fixed axis system 0 and a vehicle-fixed axis system C (located at the center of gravity) are defined in order to derive the kinematics and dynamics of the SHM model.

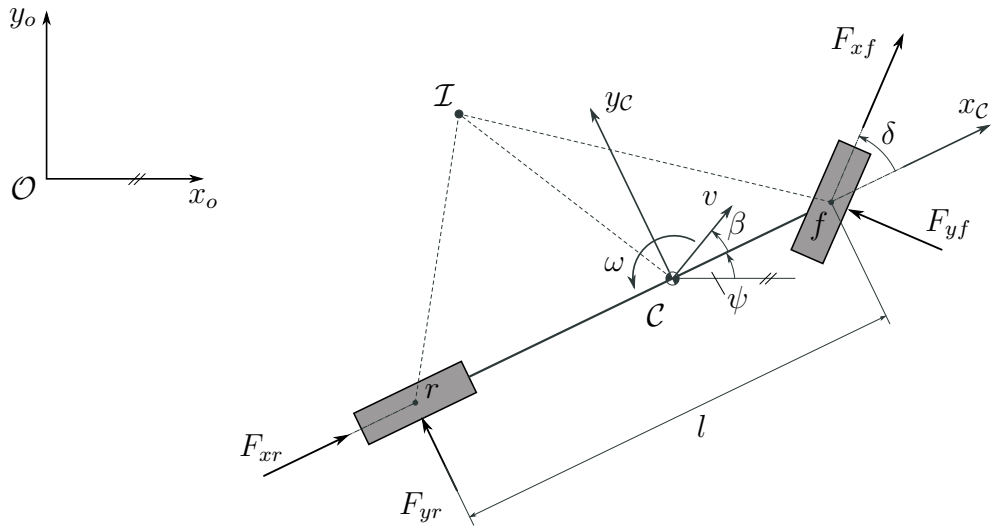

Figure 11: SHM during steady-state cornering at high speeds.

2.1.1 Kinematics

Using the axis systems defined before, see Figure 11, the velocity and the angular velocity of the SHM expressed in C are obtained via

$$\boldsymbol{v}_{0i,C} = \begin{bmatrix} v\cos\beta \\ v\sin\beta \\ 0 \end{bmatrix} \quad \text{and} \quad \boldsymbol{\omega}_{0C,C} = \begin{bmatrix} 0 \\ 0 \\ \dot{\psi} \end{bmatrix}, \tag{2-4}$$

where β is the sideslip angle measured at the the center of gravity C and $\dot{\psi}$ is the yaw angular velocity of the SHM model. Additionally, the contact point velocities at each centered wheel are calculated via

$$\boldsymbol{v}_{0j,C} = \boldsymbol{v}_{0j,C} + \boldsymbol{\omega}_{0C,C} \times \boldsymbol{r}_{Cj,C}, \tag{2-5}$$

where $j = \{f, r\}$ represents the contact point of the front and rear centered wheel respectively and, $\boldsymbol{r}_{Ci,C}$ is its position vector expressed in C. Finally, using the Equations (2-4) and (2-5), the contact points velocities are obtained as follows

$$\boldsymbol{v}_{0f,C} = \begin{bmatrix} v\cos\beta \\ v\sin\beta + \dot{\psi}l_f \\ 0 \end{bmatrix} \quad \text{and} \quad \boldsymbol{v}_{0r,C} = \begin{bmatrix} v\cos\beta \\ v\sin\beta - \dot{\psi}l_r \\ 0 \end{bmatrix}. \tag{2-6}$$

This contact point velocities are needed to compute the degree of slip, specifically the lateral tire slip, of each substitute centered wheel of the SHM.

2.1.2 Equations of motion

In order to derive the equations of motion, the acceleration of the SHM need to be derived. In this model, it is assumed small sideslip angles, i.e. $\beta \ll 1$ and consequently, the Equation (2-4) can be simplified to

$$\boldsymbol{v}_{0i,C} = \begin{bmatrix} v \\ |v|\beta \\ 0 \end{bmatrix}, \tag{2-7}$$

and the Equation ((2-6)) to

$$\boldsymbol{v}_{0f,C} = \begin{bmatrix} v \\ |v|\beta + \dot{\psi}l_f \\ 0 \end{bmatrix} \quad \text{and} \quad \boldsymbol{v}_{0r,C} = \begin{bmatrix} v \\ |v|\beta - \dot{\psi}l_r \\ 0 \end{bmatrix}. \tag{2-8}$$

Then, doing the time derivation of Equation (2-7), the acceleration is com-

puted as

$$\boldsymbol{a}_{0C,C} = \dot{\boldsymbol{v}}_{0C,C} + \boldsymbol{\omega}_{0C,C} \times \boldsymbol{v}_{0i,C} = \begin{bmatrix} 0 \\ v\dot{\psi} + |v|\dot{\beta} \\ 0 \end{bmatrix} \tag{2-9}$$

where the constant speed $\dot{v} = 0$ was assumed and higher order terms were omitted. Also the angular acceleration of the SHM is obtained via

$$\boldsymbol{\alpha}_{0C,C} = \dot{\boldsymbol{\omega}}_{0C,C} = \begin{bmatrix} 0 \\ 0 \\ \ddot{\psi} \end{bmatrix}. \tag{2-10}$$

Lateral tire forces

As mentioned before, the lateral acceleration must be considered during steady-state cornering at high speeds. Thus, the centrifugal force should be compensated by lateral forces, generated by the deformation of the contact patch see Figure 7, at the substitute tires in order to perform a curve. Therefore, small lateral sliding motions occur at the tire contact points (f, r) and in consequence, it can be assumed that the tires operate in its linear region. Then, it is possible to compute the lateral forces at each centered wheel via

$$F_{yf} = K_f s_{yf} \quad \text{and} \quad F_{yr} = K_r s_{yr}, \tag{2-11}$$

where s_{yf} and s_{yr} represent the lateral slips at the front and rear contact points respectively; K_f and K_r represent the cornering stiffness of the front and rear axle. In addition, even if the tires are equal, K_f and K_r could be different due to its dependency of wheel load and also of the suspension configuration. Therefore, computing the correct cornering stiffness brings a proper SHM model and in consequence, a correct analysis of the lateral dynamics, at low lateral accelerations, can be realized.

Lateral tire slips

The lateral tire slip s_y is defined as

$$s_y = -\frac{v_{ty}}{|r_D \Omega|}, \tag{2-12}$$

where v_{ty} represent the lateral tire velocity, r_D is the static tire radius and Ω is the wheel angular velocity. Moreover, the SHM model is not accelerating or decelerating. Therefore, the wheels are in a rolling condition, i.e. $r_D \Omega = \boldsymbol{v}_{tx}$, where $\boldsymbol{v}_{tx}$ is the longitudinal tire velocity. In addition, the components $\boldsymbol{v}_{tx}$ and v_{ty} can be computed projecting the contact point velocity into the tire longitudinal and lateral axis respectively via

$$v_{tx} = \boldsymbol{e}_{tx}^T \boldsymbol{v}_{i,C} \quad \text{and} \quad v_{ty} = \boldsymbol{e}_{ty}^T \boldsymbol{v}_{i,C}, \tag{2-13}$$

where $v_{i,C}$ represents the contact point velocity that are defined in Equation (2-8); $\boldsymbol{e}_{tx}$ and $\boldsymbol{e}_{ty}$ are the tire longitudinal and lateral unit vectors respectively, and are calculated for the front and rear substitute tires as follows

$$\begin{aligned} \text{front:} \quad \boldsymbol{e}_{tx} &= \begin{bmatrix} \cos\delta \\ \sin\delta \\ 0 \end{bmatrix}, \quad \boldsymbol{e}_{ty} = \begin{bmatrix} -\sin\delta \\ \cos\delta \\ 0 \end{bmatrix} \\ \text{rear:} \quad \boldsymbol{e}_{tx} &= \begin{bmatrix} 1 \\ 0 \\ 0 \end{bmatrix}, \qquad \boldsymbol{e}_{ty} = \begin{bmatrix} 0 \\ 1 \\ 0 \end{bmatrix} \end{aligned} \tag{2-14}$$

Finally, using Equations (2-8), (2-12), (2-13) and (2-14), we obtain the lateral slip of the front centered wheel, s_{yf}, via

$$s_{yf} = \frac{v\sin\delta - \cos\delta(|v|\beta + l_f\dot{\psi})}{|v\cos\delta + \sin\delta(|v|\beta + l_f\dot{\psi})|},$$

and also, the lateral slip s_{yr} of the rear centered wheel as

$$s_{yr} = -\frac{|v|\beta - l_r\dot{\psi}}{|v|}$$

then, assuming small steering wheel angles $\delta < 0.2$ and also, small yaw angular velocities $\dot{\psi}$, i.e. $|l_f\dot{\psi}| \ll |v|$ and $|l_r\dot{\psi}| \ll |v|$, the lateral slips were reduced to

$$s_{yf} = -\beta - \frac{l_f}{|v|}\dot{\psi} + \frac{v}{|v|}\delta \quad \text{and} \quad s_{yr} = -\beta + \frac{l_r}{|v|}\dot{\psi}\ . \tag{2-15}$$

Finally, the equations of motion of the SHM model are described by its lateral dynamics, i.e in the y-axis, via

$$m\left(v\dot{\psi} + |v|\dot{\beta}\right) = F_{yf} + F_{yr}, \tag{2-16}$$

and also with its yaw rate dynamics, i.e. around the z-axis, as

$$\Theta\ddot{\psi} = l_f F_{yf} - l_r F_{yr}, \tag{2-17}$$

where m and Θ represents the mass and the moment of inertia (z-axis) of the SHM respectively. Finally, considering the linear tire model defined by Equation (2-11) and the lateral slips defined by Equation (2-15), in the equations of motion (2-16) and (2-17) were obtained

$$\begin{aligned}\dot{\beta} &= \frac{K_f}{m|v|}\left(-\beta - \frac{l_f}{|v|}\dot{\psi} + \frac{v}{|v|}\delta\right) + \frac{K_r}{m|v|}\left(-\beta + \frac{l_r}{|v|}\dot{\psi}\right) - \frac{v}{|v|}\dot{\psi} \\ \ddot{\psi} &= \frac{l_f K_f}{\Theta}\left(-\beta - \frac{l_f}{|v|}\dot{\psi} + \frac{v}{|v|}\delta\right) - \frac{l_r K_r}{\Theta}\left(-\beta + \frac{l_r}{|v|}\dot{\psi}\right).\end{aligned} \tag{2-18}$$

In addition, these equations can be represented by a space-state equation as follows

$$\begin{aligned}\begin{bmatrix}\dot{\beta}\\ \ddot{\psi}\end{bmatrix} &= \begin{bmatrix}-\frac{K_f+K_r}{m|v|} & \frac{l_rK_r - l_fK_f}{m|v||v|} - \frac{v}{|v|}\\ \frac{l_rK_r - l_fK_f}{\Theta} & -\frac{l_f^2K_f + l_r^2K_r}{\Theta|v|}\end{bmatrix}\begin{bmatrix}\beta\\ \dot{\psi}\end{bmatrix} + \begin{bmatrix}\frac{v}{|v|}\frac{K_f}{m|v|}\\ \frac{v}{|v|}\frac{l_fK_f}{\Theta}\end{bmatrix}\delta \\ \underbrace{\dot{\boldsymbol{x}}} &= \underbrace{\boldsymbol{A}}\ \underbrace{\boldsymbol{x}} + \underbrace{\boldsymbol{B}}\ \underbrace{\boldsymbol{u}}\end{aligned} \tag{2-19}$$

This formulation, Equation (2-19), can be used for stability, phase-plane analysis as well as for design of safety control systems, e.g. ESP and active front steering systems (AFS). In addition, this model can easily be extended for all-wheel steering vehicles, i.e. including rear wheel steering. In fact, this extended model is employed to design control strategies for four-wheel steering systems (4WS). This variant of the simple handling vehicle model is presented in Chapter 4.

The planar vehicle model presented above was derived taking into account several assumptions and simplifications. However, for advance vehicle dynamic applications, a fully non-linear and three-dimensional vehicle model is needed. This model should consider the nonlinearities of the main components that affects the behavior of passenger cars. In the followings subsections, modeling aspects of road vehicles and its subsystems are described.

2.2 Multibody vehicle model

In general, road vehicles are modeled by multibody systems [17, 33]. This is a common approach for the study of the vehicle's handling [47] and ride properties [48, 49], and also for the design of vehicle safety systems [45, 46]. The overall multibody vehicle model can be divided in different systems, e.g. the vehicle framework, steering, the power drive-train, the road and the tire, see Figure 12. The vehicle framework includes the vehicle's body or chassis and modules for the wheel/axle suspension system. In addition, external loads, the

engine and the driver/passengers can be included on the vehicle framework. For handling and ride analysis of passenger cars, the chassis can be modeled as a rigid body. However, in heavy trucks models, the chassis compliance and the driver's cabin should be considered.

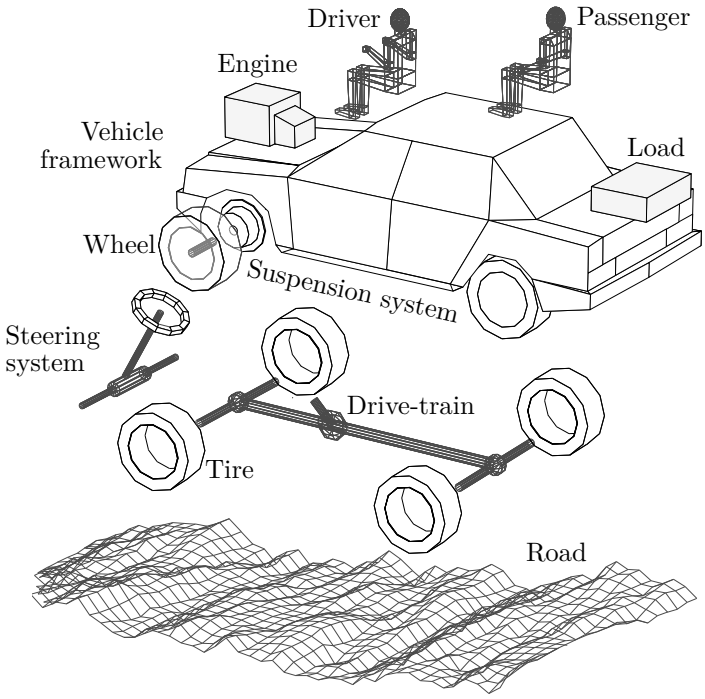

Figure 12: Multibody road vehicle model, tire and road system [33].

Besides the vehicle's framework, i.e. vehicle body, wheel/axle suspension system, steering system and power drive-train, the tire-road interaction plays an essential role in road vehicles. In fact, this interaction generates the necessary forces to move the car. In the next subsections, a modeling aspect of the wheel/axle suspension, tire and road system is presented.

2.2.1 Modeling considerations

In this thesis, nine rigid bodies are employed to model the road vehicle dynamics, i.e. one chassis, four knuckles and four wheels (tire + rim). In addition, some reference axis systems are also defined to describe the motion of the bodies. In Figure 13, the rigid bodies and their axis systems as well as the earth-fixed axis system with origin O are illustrated. The vehicle axis system V, located at the middle of the front axle, is defined by ISO Standard 8855, i.e. with positive x_V in the forward direction, positive y_V to the driver's left and positive z_V up. In addition, each wheel-fixed axis system is located at the geometric center of its respective knuckle.

In total, this multibody vehicle model has 14 degrees of freedom (DOF). The DOF include the vehicle's body translations $\{x_V, y_V, z_V\}$; the vehicle's body rotations $\{\alpha, \beta, \gamma\}$; the wheels' vertical displacements $\{z_1, z_2, z_3, z_4\}$ as well as their spin speeds $\{\omega_1, \omega_2, \omega_3, \omega_4\}$. Furthermore, the subscripts {1,2,3,4} indicate the front left, front right, rear left and rear right wheels respectively.

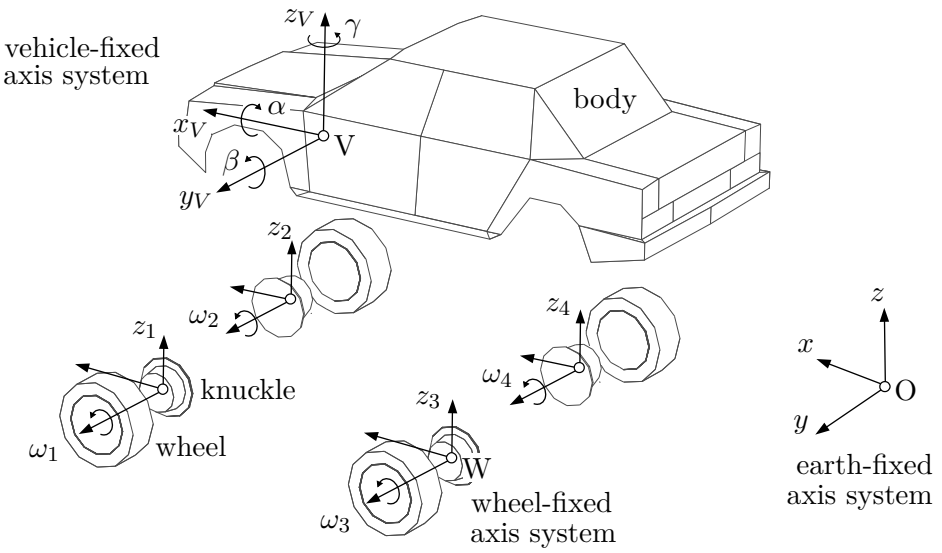

Figure 13: Degrees of freedom (DOF) of the multibody road vehicle model. Graphic representation modified from [33].

2.2.2 Suspension system

The suspension is one of the most important mechanical subsystems in road vehicles. This system connects each wheel's body to the chassis through mechanical and force elements. Some functionalities of the suspension system involves:

- carry the vehicle's weight,
- maintain a correct wheel alignment,
- ensure a good contact between the tire and the road,
- reduce the effect of road impacts.

Suspension systems include elements such as guiding elements, e.g. control arms and linkages, and also force elements, e.g. damper, air spring, coil spring, anti-roll bars and bushings. Some of the most common suspension systems in passenger cars are the double wishbone, the McPherson and the multi-link suspension system, see Figure 14. For the derivation of the wheel/axle suspension model, the double wishbone suspension layout is

considered in this section. The derivation of a wheel/axle suspension model is discussed in this section (exemplary on the double wishbone suspension). Other types of suspension models are can be found in [33, 67].

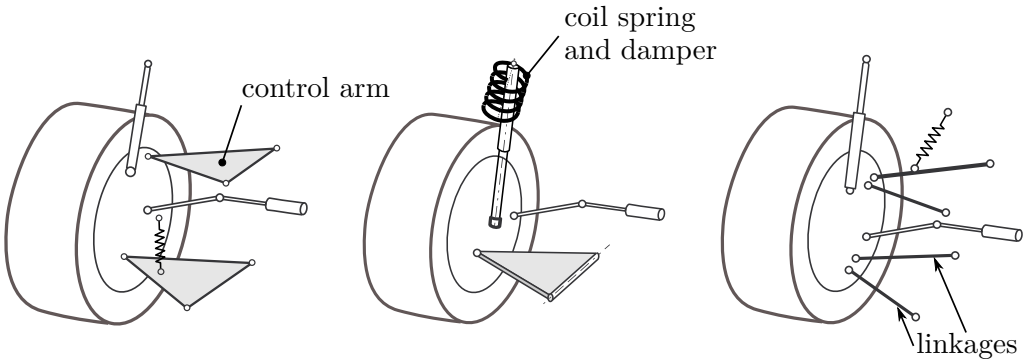

Figure 14: Multipurpose suspension systems: double wishbone, McPherson and multi-link.

Wheel body position and orientation

The vehicle-fixed axis system V is considered as the reference coordinate system for the suspension kinematic model. Figure 15 illustrates the double wishbone suspension layout, its main components as well as the wheel-fixed axis system W (located at the geometric center of the wheel's body).

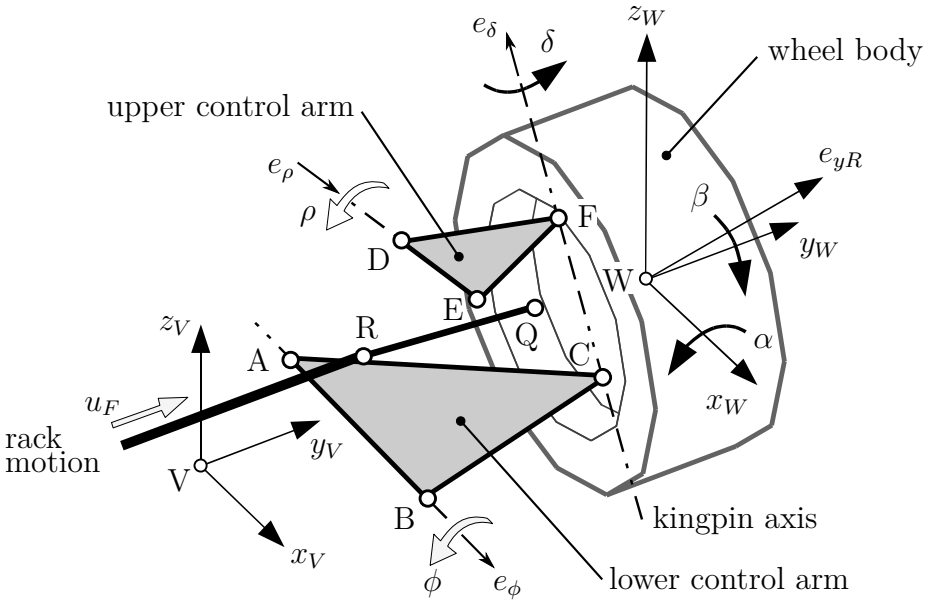

Figure 15: Double wishbone suspension layout (front left) and components. The graphic depiction was modified from [33].

This suspension kinematics depends of two motions. The first one is related to the wheel up/down displacement or the rotation of the lower control

arm ϕ. The second motion is due to the rack displacement u_F (front axle). Therefore, using these variables it is possible to describe the whole suspension kinematics, i.e. ϕ and u_F are the the generalized coordinates.

Taking into consideration the suspension layout depicted above, it is possible to obtain the wheel's body position via

$$\boldsymbol{r}_{VW,V} = \boldsymbol{r}_{VB,V} + \boldsymbol{A}_{\phi}\boldsymbol{r}_{BC,\phi} + \boldsymbol{A}_{VW}\boldsymbol{r}_{CW,W} \tag{2-20}$$

where $\boldsymbol{A}_{\phi}$ and $\boldsymbol{A}_{VW}$ represent the rotation matrices of the lower control arm and the wheel body relative vehicle-fixed axis system V, respectively. In addition, the subscripts $_{,V}$ and $_{,W}$, define in which axis system the vector is measured. In the case of the subscript $_{,\phi}$, it defines a vector measured in an axis system fixed to the lower control arm.

The set of positions of the bushings (A, B, D, E), the ball joints (C, F, R, Q) and the wheel design position W are often called "hardpoints", and they define the topology of the suspension. Moreover, the rotation matrix of the lower control arm $\boldsymbol{A}_{\phi}$ can be calculated using its axis of rotation $\boldsymbol{e}_{\phi}$ (defined by bushings A and B) as follows

$$\boldsymbol{A}_{\phi} = \boldsymbol{e}_{\phi}\boldsymbol{e}_{\phi}^{T} + \left(\boldsymbol{I}_{3\times3} - \boldsymbol{e}_{\phi}\boldsymbol{e}_{\phi}^{T}\right)\cos\phi + \widetilde{\boldsymbol{e}}_{\phi}\sin\phi, \tag{2-21}$$

where ϕ is the angle of rotation around $\boldsymbol{e}_{\phi}$, $\boldsymbol{I}_{3\times3}$ is a 3×3 identity matrix, and $\widetilde{\boldsymbol{e}}_{\phi}$ is the skew-symmetric matrix defined by the components of $\boldsymbol{e}_{\phi}$. This type of formulation [50] is convenient because the rotation axis of the lower control arm $\boldsymbol{e}_{\phi}$ is defined by the topology of the suspension.

The rotation matrix of the wheel body $\boldsymbol{A}_{VW}$ depends of the rotation angle δ around the kingpin axis $\boldsymbol{e}_{\delta}$. In addition, the orientation of this axis can be obtained by two elementary rotations, i.e. around the $x_W(\alpha)$ and $y_W(\beta)$ axis. Finally, the rotation around the kingpin axis δ is commanded by the rack displacement u_F. Consequently, the rotation matrix $\boldsymbol{A}_{VW}$ can be calculated by successive rotation as

$$\boldsymbol{A}_{VW} = \boldsymbol{A}_{\alpha}\boldsymbol{A}_{\beta}\boldsymbol{A}_{\delta}, \tag{2-22}$$

where

$$\boldsymbol{A}_{\alpha} = \begin{bmatrix} 1 & 0 & 0 \\ 0 & \cos\alpha & -\sin\alpha \\ 0 & \sin\alpha & \cos\alpha \end{bmatrix}, \; \boldsymbol{A}_{\beta} = \begin{bmatrix} \cos\beta & 0 & \sin\beta \\ 0 & 1 & 0 \\ -\sin\beta & 0 & \cos\beta \end{bmatrix} \tag{2-23}$$

$$\boldsymbol{A}_{\delta} = \boldsymbol{e}_{\delta}\boldsymbol{e}_{\delta}^{T} + \left(\boldsymbol{I}_{3\times3} - \boldsymbol{e}_{\delta}\boldsymbol{e}_{\delta}^{T}\right)\cos\delta + \widetilde{\boldsymbol{e}}_{\delta}\sin\delta.$$

In order to derive the position and orientation of the wheel's body in

function of the generalized coordinates, i.e. ϕ and u_F, kinematic constraints need to be considered.

Constraint equation: wheel up/down motion

The first kinematic constraint equation is related to the lower and upper control arms. In order to calculate the rotation angle of the upper control arm ρ in function of the generalized coordinate ϕ, a pure wheel up/down motion is considered as illustrated in the Figure 16.

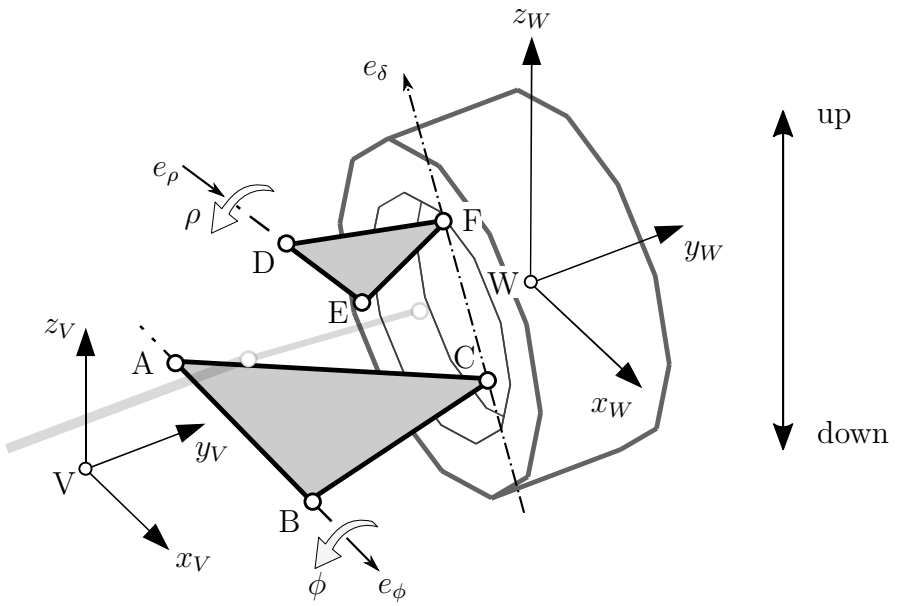

Figure 16: Basic representation of a pure wheel up/down motion for a double wishbone suspension system.

The position of the ball joint F can be calculated using the rotation matrix of the lower control arm $\boldsymbol{A}_\phi$ via

$$\boldsymbol{r}_{VF,V} = \boldsymbol{r}_{VB,V} + \boldsymbol{A}_\phi \boldsymbol{r}_{BC,\phi} + \boldsymbol{A}_{VW} \boldsymbol{r}_{CF,W} \tag{2-24}$$

or by using the rotation matrix of the upper control arm $\boldsymbol{A}_\rho$ as

$$\boldsymbol{r}_{VF,V} = \boldsymbol{r}_{VD,V} + \boldsymbol{A}_\rho \boldsymbol{r}_{DF,\rho} \tag{2-25}$$

Then, by using Equation (2-24) and (2-25), the first constraint equation if defined as follows

$$\boldsymbol{r}_{VB,V} + \boldsymbol{A}_\phi \boldsymbol{r}_{BC,\phi} + \boldsymbol{A}_{VW} \boldsymbol{r}_{CF,W} = \boldsymbol{r}_{VD,V} + \boldsymbol{A}_\rho \boldsymbol{r}_{DF,\rho} \tag{2-26}$$

Therefore, by solving the constraint Equation (2-26), it is possible to find expressions for the elementary rotation angles of $\boldsymbol{A}_{VW}$, i.e. α and β, and for

the rotation of the upper control arm ρ in terms of ϕ. These expression can be written as follows

$$\alpha = \alpha(\phi),\ \beta = \beta(\phi) \text{ and } \rho = \rho(\phi) \tag{2-27}$$

As consequence of the previous equation, the elementary rotation matrices can be written as

$$\boldsymbol{A}_\alpha = \boldsymbol{A}_\alpha(\phi) \text{ and } \boldsymbol{A}_\beta = \boldsymbol{A}_\beta(\phi). \tag{2-28}$$

In addition, the rotation matrix $\boldsymbol{A}_\delta$ depends of $\boldsymbol{e_\delta}$ and the orientation of this axis depends of ϕ, therefore, $\boldsymbol{A}_\delta = \boldsymbol{A}_\delta(\phi)$. Finally, Equation (2-22) can be rewritten as function of ϕ, i.e. for pure wheel up/down motions, as

$$\boldsymbol{A}_{VW} = \boldsymbol{A}_\alpha(\phi)\boldsymbol{A}_\beta(\phi)\boldsymbol{A}_\delta(\phi) \tag{2-29}$$

and consequently, the position of the wheel's body relative to the vehicle-fixed axis system V (Equation (2-20)) is also function of ϕ. Details about the derivation of the expressions $\alpha = \alpha(\phi)$, $\beta = \beta(\phi)$ and $\rho = \rho(\phi)$ can be found in Appendix A.1.

Constraint equation: rack displacement

For the suspension model presented here, a pure lateral rack motion was assumed. The second constraint equation is related to the drag link (defined by the ball joint R and Q). From Figure 17 and considering pure lateral rack motions, the position of the ball joint R can be calculated via

$$\boldsymbol{r}_{VR,V} = \boldsymbol{r}^d_{VR,V} + \begin{bmatrix} 0 \\ u_F \\ 0 \end{bmatrix}. \tag{2-30}$$

where $r^d_{VR,V}$ is the design position of the joint R and is defined by the suspension topology, and u_F is the rack displacement. In addition, for rear wheel steering vehicles, the rear rack displacement u_R needs to be considered in the rear suspension kinematic models. The position of the ball joint Q can be computed using the lower control arm rotation matrix A_ϕ as follows

$$\boldsymbol{r}_{VQ,V} = \boldsymbol{r}_{VA,V} + \boldsymbol{A}_\phi \boldsymbol{r}_{AC,\phi} + \boldsymbol{A}_{VW}\boldsymbol{r}_{CQ,W} \tag{2-31}$$

The drag link is supposed to be a rigid linkage of length l_{RQ} and therefore, the second constraint can be defined as

$$(\boldsymbol{r}_{VQ,V} - \boldsymbol{r}_{VR,V})^T (\boldsymbol{r}_{VQ,V} - \boldsymbol{r}_{VR,V}) = l_{RQ}^2 \tag{2-32}$$

Finally, by using Equation (2-29), (2-30), (2-31) and (2-32), it is possible to find an expression of the wheel's body rotation δ around the kingpin axis e_δ in function of the rack motion u_F, i.e. $\delta = \delta(u_F)$. Therefore, the rotation matrix A_δ is also function of u_F and can be expressed as

$$\boldsymbol{A}_\delta = \boldsymbol{A}_\delta(\phi, u_F) \tag{2-33}$$

where the influence of the wheel up/down motion ϕ was also considered. Details about the derivations of $\boldsymbol{A}_\delta(\phi, u_F)$ can be found in Appendix A.2.

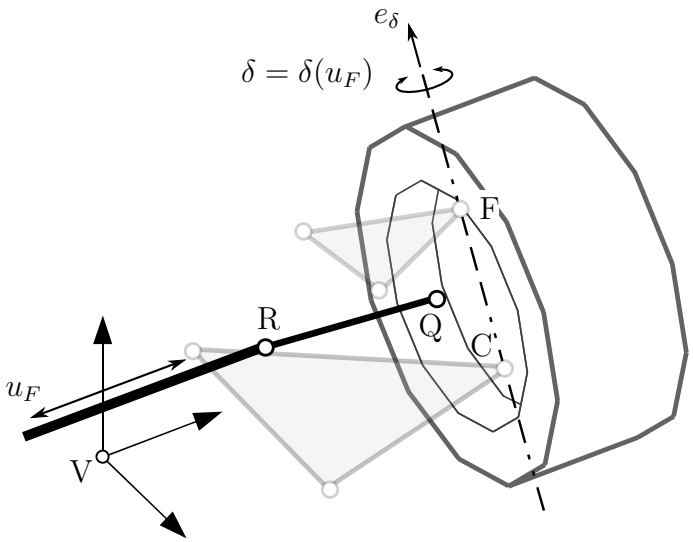

Figure 17: Basic representation of a pure lateral rack motion for a double wishbone suspension system.

Then, the wheel's body position (Equation (2-20)) can be expressed in function of the generalized coordinates ϕ and u_F as follows

$$\boldsymbol{r}_{VW,V}(\phi, u_F) = \boldsymbol{r}_{VB,V} + \boldsymbol{A}_\phi(\phi)\boldsymbol{r}_{BC,\phi} + \boldsymbol{A}_{VW}(\phi, u_F)\boldsymbol{r}_{CW,W} \tag{2-34}$$

where

$$\boldsymbol{A}_{VW}(\phi, u_F) = \boldsymbol{A}_\alpha(\phi)\boldsymbol{A}_\beta(\phi)\boldsymbol{A}_\delta(\phi, u_F) \tag{2-35}$$

Because the wheel's position is function of ϕ and u_F, its velocity is also function of the generalized coordinates. By taking the time derivative of Equation (2-34), one gets

$$\dot{\boldsymbol{r}}_{VW,V}(\phi, u_F) = \frac{\partial \dot{\boldsymbol{r}}_{VW,V}}{\partial \dot{\phi}} \dot{\phi} + \frac{\partial \dot{\boldsymbol{r}}_{VW,V}}{\partial \dot{u}_F} \dot{u}_F \tag{2-36}$$

On the order hand, the wheel's body angular velocity can be calculated via

$$\boldsymbol{\omega}_{VW}(\phi, u_F) = \frac{\partial \boldsymbol{\omega}_{VW}}{\partial \dot{\phi}} \dot{\phi} + \frac{\partial \boldsymbol{\omega}_{VW}}{\partial \dot{u}_F} \dot{u}_F \tag{2-37}$$

A physical interpretation of the partial derivatives of the wheel's body velocity and angular velocity respect to the generalized speeds, i.e. $\dot{\phi}$ and $\dot{u}_F$, presented in Equation (2-36) and (2-37) could be, how the tire forces (generated in the tire-road contact area) are transfered to the vehicle's body through the suspension system.

Following the same modeling process presented above, it is possible to model complex suspension systems like multi-link or even a Formula 1 suspension concept, e.g. push-rod and pull-rod suspension systems.

2.2.3 Tire modeling

The tires are complex and essential elements in road vehicles. They are responsible to transmit the engine power to the road and consequently, generate the necessary forces to move the car, e.g. accelerate/braking the vehicle or negotiate a curve. These forces are created in the contact patch, i.e. the contact area between the tire and the road surface. In the current literature, there are two main approaches for tire modeling, i.e. empirical and physical. The first approach uses mathematical functions to fit experimental tire force curves [54]. In spite of matching these data extremely well, these tire models do not offer a physical meaning of its empirical parameters. In the other hand, tire models based on finite element methods are physical models that are employed commonly for high frequency analysis, e.g. vehicle comfort simulations under uneven roads. These tire models are computer time consuming and need a large number of experimental data. Consequently, they are too complicated to be used in vehicle handling simulations. However, a simplification of these types of models can make them suitable for multibody vehicle applications [51].

TMeasy [33], is a semi-physical tire model that uses a small number of parameters to characterize the tire-road contact forces. These forces are applied on the contact point and TMeasy estimate them with a sophisticated but quite simple contact point calculation [52]. In addition, the parameters of the TMeasy tire model has physical meaning and therefore, an engineering parameter estimation is possible [53]. In Figure 18, a tire-road contact representation is depicted. The vector $\boldsymbol{r}_{0M}$ and $\boldsymbol{e}_{yR}$ defines the wheel's position and

orientation in relation to the earth-fixed axis system. In addition, the local road plane $z = z(x, y)$ can be defined by a road point P_0 and a unit vector perpendicular to this plane $\boldsymbol{e}_n$, as can be seen in the right side of Figure 18.

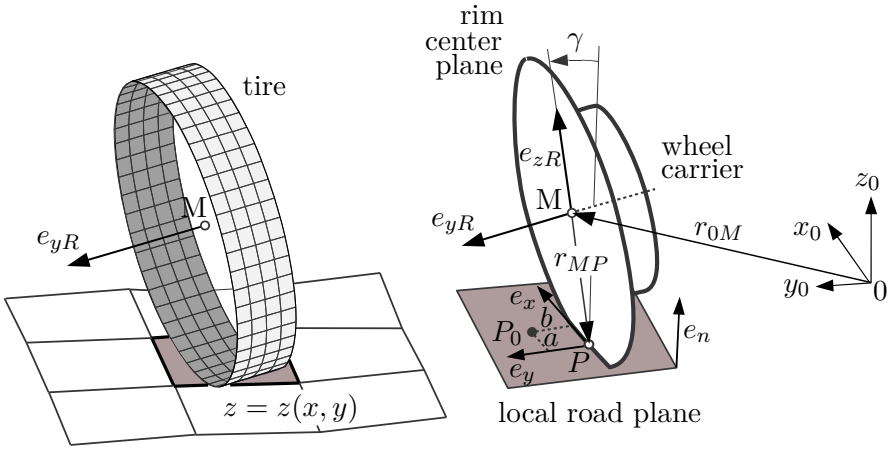

Figure 18: TMeasy contact point and local plane geometry [53].

The longitudinal, lateral and radial tire directions can be computed via

$$\boldsymbol{e}_x = \frac{\boldsymbol{e}_{yR} \times \boldsymbol{e}_n}{|\boldsymbol{e}_{yR} \times \boldsymbol{e}_n|},\ \boldsymbol{e}_y = \boldsymbol{e}_n \times \boldsymbol{e}_x \quad \text{and} \quad \boldsymbol{e}_{zR} = \boldsymbol{e}_x \times \boldsymbol{e}_{yR}, \tag{2-38}$$

respectively. Moreover, $\boldsymbol{e}_x$ was normalized because $\boldsymbol{e}_{yR}$ is not perpendicular (in general) to the road normal vector $\boldsymbol{e}_n$. This deviation is defined by the tire camber angle γ and then, a first but quite realistic approximation of the contact point P is obtained by

$$\boldsymbol{r}_{MP,0} = -r_S \boldsymbol{e}_{zR}, \tag{2-39}$$

where r_S is the static tire radius and $\boldsymbol{e}_{zR}$ was defined in Equation (2-38). More details about the contact point calculation can be found in [52].

In normal driving maneuvers, e.g. acceleration or deceleration in a curve, the longitudinal slip s_x and lateral slip s_y occur at the same time. Therefore, the combination of slips and thus of the longitudinal and lateral forces should be handled by the tire model. In order to achieve the contribution of longitudinal and lateral slips to the combined slip, with a similar weight, TMeasy performs a normalization process as follows:

$$s = \sqrt{\left(\frac{s_x}{\hat{s}_x}\right)^2 + \left(\frac{s_y}{\hat{s}_y}\right)^2} = \sqrt{\left(s_x^N\right)^2 + \left(s_y^N\right)^2} \tag{2-40}$$

where s_x^N and s_y^N are the normalized slips. Furthermore, the normalizing factors $\hat{s}_x$ and $\hat{s}_y$ take into account the longitudinal and lateral force characteristics and are defined via

$$\hat{s}_i = \frac{s_i^M}{s_x^M + s_y^M} + \frac{F_i^M/dF_i^0}{F_x^M/dF_x^0 + F_y^M/dF_y^0}, \quad i = \{x, y\}. \tag{2-41}$$

Similar to the curve of longitudinal and lateral forces, the combined force $F = F(s)$ can be defined by their characteristic parameters dF^0, s^M, F^M, s^S, and F^S. These parameters are defined as:

$$\begin{aligned} dF^0 &= \sqrt{(dF_x^0 \hat{s}_x \cos\phi)^2 + (dF_y^0 \hat{s}_y \sin\phi)^2} \\ s^M &= \sqrt{\left(\tfrac{s_x^M}{\hat{s}_x}\cos\phi\right)^2 + \left(\tfrac{s_y^M}{\hat{s}_y}\sin\phi\right)^2} \\ F^M &= \sqrt{(F_x^M \cos\phi)^2 + \left(F_y^M \sin\phi\right)^2} \\ s^S &= \sqrt{\left(\tfrac{s_x^S}{\hat{s}_x}\cos\phi\right)^2 + \left(\tfrac{s_y^S}{\hat{s}_y}\sin\phi\right)^2} \\ F^S &= \sqrt{(F_x^S \cos\phi)^2 + \left(F_y^S \sin\phi\right)^2}. \end{aligned} \tag{2-42}$$

The angular function ϕ is used to grant a smooth transition from the longitudinal and lateral force to the combined force. Finally, the longitudinal and lateral resulting forces are derived from the combined force as follows:

$$F_x = F\cos(\phi),\ F_y = F\sin(\phi) \quad \text{where} \quad \cos(\phi) = \frac{s_x^N}{s},\ \sin(\phi) = \frac{s_y^N}{s}. \tag{2-43}$$

Figure 19 shows the mutual influence of longitudinal and lateral forces against the longitudinal and lateral slips, computed by TMeasy, for a standard commercial tire. Details of the tire characteristics are presented in Table 1.

Table 1: TMeasy tire model parameters for a tire of type Radial 205/50R15

	Parameter	Value	Unit
Long.	dF_x^0	69000	N/-
	s_x^M	0.16	-
	F_x^M	3100	N
	s_x^S	0.5	-
	F_x^S	2800	N
Lat.	dF_y^0	66000	N/-
	s_y^M	0.205	-
	F_y^M	2950	N
	s_x^S	0.5	-
	F_y^S	2800	N

The lateral and longitudinal combined tire forces at different values of longitudinal and lateral slips are illustrated in Figure 20.

2.2.4

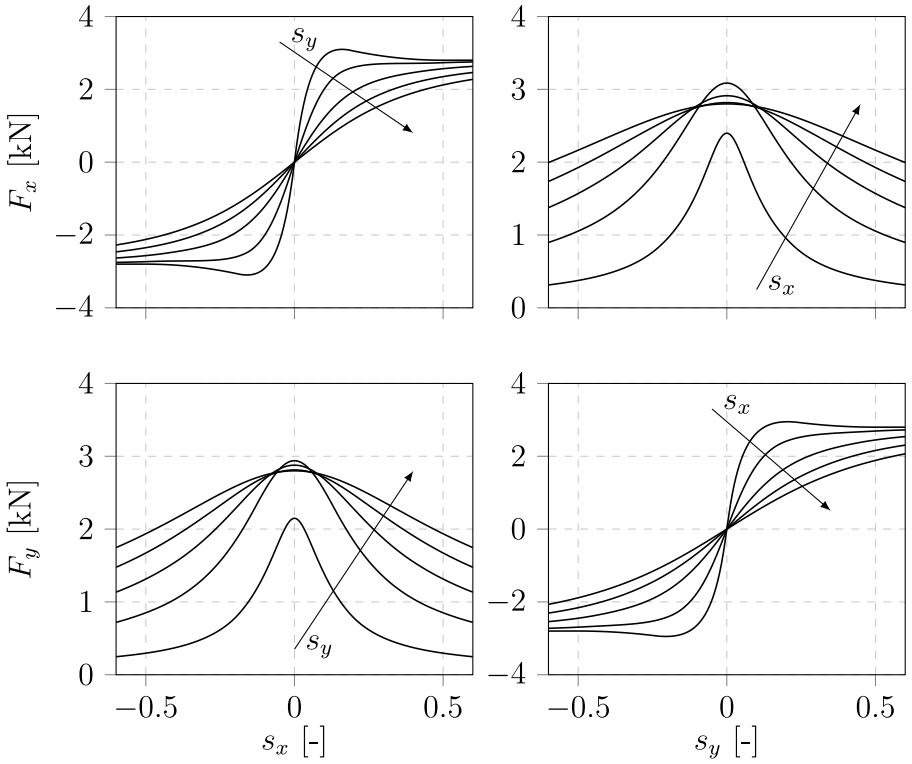

Figure 19: Relationship between forces and slips of a passenger tire computed by TMeasy [33].

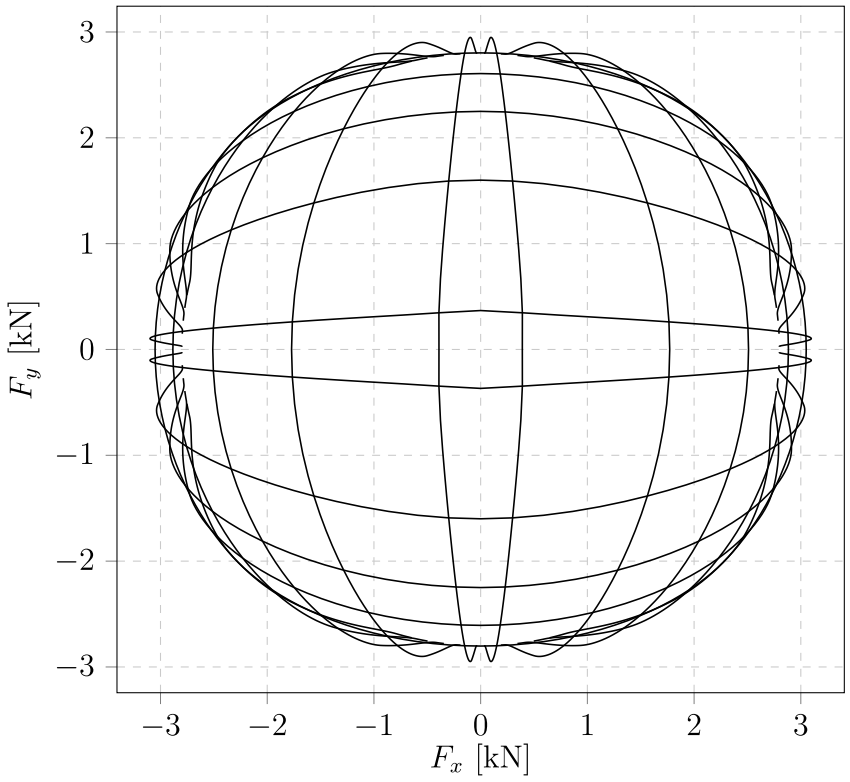

Figure 20: Combined forces at different slips.

Kinematics

In order to describe the position, velocity and acceleration of a mechanical system, a set of appropriate axis systems are required. Additionally to the reference frames presented in Figure 13, a chassis-fixed axis system C is also considered as shown in Figure 21. This axis system is defined by the chassis mass distribution. Details of each reference frame are summarized in Table 2. In addition, it is assumed that the geometric center of the knuckle and wheel are close enough and in consequence, an unique axis system is used for both bodies, i.e. W_i, where i denotes one of the four wheels.

Table 2: Reference frames of the proposed multibody vehicle model.

Reference frame	Origin of frame	Unit base vectors orientation
Inertial frame	O: earth-fixed	x, y : horizontal plane z : up (opposite to the gravity)
Body-fixed frame	C: chassis center of mass	x : forward
Moving frame	V: middle of the front axle	y : driver's left
Body-fixed frame	i: wheel and knuckle center	z : up

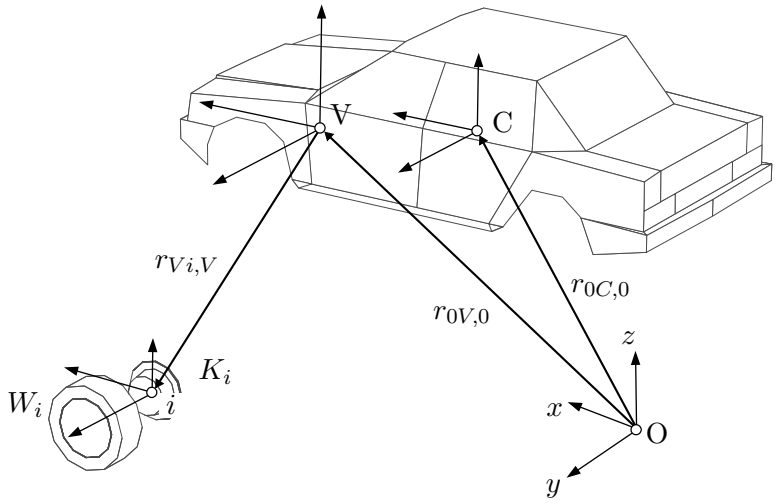

Figure 21: Reference frames employed to describe the kinematics of the multibody vehicle model proposed in this thesis.

Position and orientation

Vehicle-fixed axis system V – The position of the vehicle-fixed axis system V relative to the earth-fixed axis system O is calculated as follows

$$\boldsymbol{r}_{0V,0} = [x\ y\ z]^T \tag{2-44}$$

and its orientation via

$$\boldsymbol{A}_{0V} = \boldsymbol{A}_{\gamma}\boldsymbol{A}_{\beta}\boldsymbol{A}_{\alpha} \tag{2-45}$$

where γ (yaw), β (pitch) and α (roll) are the elementary rotation around the $z-$, $y-$ and $x-$ axis of V respectively, and are defined as

$$\boldsymbol{A}_{\gamma} = \begin{bmatrix} \cos\gamma & -\sin\gamma & 0 \\ \sin\gamma & \cos\gamma & 0 \\ 0 & 0 & 1 \end{bmatrix}, \boldsymbol{A}_{\beta} = \begin{bmatrix} \cos\beta & 0 & \sin\beta \\ 0 & 1 & 0 \\ -\sin\beta & 0 & \cos\beta \end{bmatrix}, \boldsymbol{A}_{\alpha} = \begin{bmatrix} 1 & 0 & 0 \\ 0 & \cos\alpha & -\sin\alpha \\ 0 & \sin\alpha & \cos\alpha \end{bmatrix}. \tag{2-46}$$

Chassis-fixed axis system C – The chassis position C and orientation can be obtained via

$$\boldsymbol{r}_{0C,0} = \boldsymbol{r}_{0V,0} + \boldsymbol{A}_{0V}\boldsymbol{r}_{VC,V} \quad \text{and} \quad \boldsymbol{A}_{0C} = \boldsymbol{A}_{0V} \tag{2-47}$$

Wheel-fixed axis system W – The position of the wheel i, are given by

$$\boldsymbol{r}_{0i,0} = \boldsymbol{r}_{0V,0} + \boldsymbol{A}_{Vi}\boldsymbol{r}_{Vi,V} \tag{2-48}$$

and its orientation via

$$\boldsymbol{A}_{0i} = \boldsymbol{A}_{0V}\boldsymbol{A}_{Vi} \tag{2-49}$$

The position and orientation of the wheel i relative to the vehicle-fixed axis system V, i.e. $\boldsymbol{r}_{Vi,V}$ and $\boldsymbol{A}_{Vi}$, are defined by the up/down wheel's motion z_i or by the lower control arm rotation ϕ_i, and the rack displacement u as presented in the Subsection 2.2.2. Then, $\boldsymbol{r}_{Vi,V}$ can be calculated as

$$\boldsymbol{r}_{Vi,V} = \begin{cases} \boldsymbol{r}_{Vi,V}(z_i, u_F) & i = 1, 2 \,(\text{front wheels}) \\ \boldsymbol{r}_{Vi,V}(z_i, u_R) & i = 3, 4 \,(\text{rear wheels}) \end{cases} \tag{2-50}$$

and $\boldsymbol{A}_{Vi}$ via

$$\boldsymbol{A}_{Vi} = \begin{cases} \boldsymbol{A}_{Vi}(z_i, u_F) & i = 1, 2 \,(\text{front wheels}) \\ \boldsymbol{A}_{Vi}(z_i, u_R) & i = 3, 4 \,(\text{rear wheels}) \end{cases} \tag{2-51}$$

where the rear rack displacement u_R was taken into account.

Velocities

Vehicle-fixed axis system V – It is possible to express the velocity of V relative to this axis system using the Equation (2-44) and (2-45) as follows

$$\boldsymbol{v}_{0V,V} = \boldsymbol{A}_{0V}^{T}\dot{\boldsymbol{r}}_{0V,0} = \boldsymbol{A}_{0V}^{T}\begin{bmatrix} \dot{x} \\ \dot{y} \\ \dot{z} \end{bmatrix}, \tag{2-52}$$

and its angular velocity can be decomposed in elementary velocities via

$$\begin{aligned} \boldsymbol{\omega}_{0V,V} &= \begin{bmatrix} 1 \\ 0 \\ 0 \end{bmatrix} \dot{\alpha} + \begin{bmatrix} 0 \\ \cos\alpha \\ -\sin\alpha \end{bmatrix} \dot{\beta} + \begin{bmatrix} -\sin\beta \\ \sin\alpha\cos\beta \\ \cos\alpha\cos\beta \end{bmatrix} \dot{\gamma} \\ &= \begin{bmatrix} 1 & 0 & -\sin\beta \\ 0 & \cos\alpha & \sin\alpha\cos\beta \\ 0 & -\sin\alpha & \cos\alpha\cos\beta \end{bmatrix} \begin{bmatrix} \dot{\alpha} \\ \dot{\beta} \\ \dot{\gamma} \end{bmatrix}. \end{aligned} \tag{2-53}$$

Using the vehicle-fixed axis system V to derive the velocities and accelerations of the bodies is quite convenient because, for example, a simplification is possible by employing the components of $v_{0V,V}$ and $\omega_{0V,V}$ as generalized speeds. Furthermore, the suspension kinematics was already defined relative to this axis system, then the velocity and acceleration of the wheel's body can be obtained easily.

Chassis-fixed axis system C – the velocity of C relative to V is obtained deriving Equation (2-47) via

$$\dot{\boldsymbol{r}}_{0C,0} = \dot{\boldsymbol{r}}_{0V,0} + \dot{\boldsymbol{A}}_{0V}\boldsymbol{r}_{VC,V} + \boldsymbol{A}_{0V}\dot{\boldsymbol{r}}_{VC,V}, \tag{2-54}$$

then by left-multiplication with $\boldsymbol{A}_{0V}^T$, i.e. transformation in the vehicle-fixed axis system V, results in

$$\boldsymbol{v}_{0C,V} = \boldsymbol{v}_{0V,V} + \boldsymbol{\omega}_{0V,V} \times \boldsymbol{r}_{VC,V}, \tag{2-55}$$

where $\dot{\boldsymbol{r}}_{VC,V} = 0$ (constant in V) and the equivalences $\boldsymbol{A}_{0V}^T\dot{\boldsymbol{A}}_{0V} = \widetilde{\boldsymbol{\omega}}_{0V,V}$ and $\widetilde{\boldsymbol{\omega}}\boldsymbol{r} = \boldsymbol{\omega} \times \boldsymbol{r}$ were take into account. In addition, the chassis-fixed axis system C angular velocity is simply given by $\boldsymbol{\omega}_{0C,V} = \boldsymbol{\omega}_{0V,V}$.

Wheel-fixed axis system W_i – The velocity of a specific wheel's body i relative to O can be calculated by time derivative of Equation (2-48) as follows

$$\dot{\boldsymbol{r}}_{0i,0} = \dot{\boldsymbol{r}}_{0V,0} + \dot{\boldsymbol{A}}_{0V}\boldsymbol{r}_{Vi,V} + \boldsymbol{A}_{0V}\dot{\boldsymbol{r}}_{Vi,V}, \tag{2-56}$$

then by left-multiplication with A_{0V}^T results in

$$\boldsymbol{v}_{0i,V} = \boldsymbol{v}_{0V,V} + \boldsymbol{\omega}_{0V,V} \times \boldsymbol{r}_{Vi,V} + \dot{\boldsymbol{r}}_{Vi,V}, \tag{2-57}$$

where $\boldsymbol{r}_{Vi,V}$ is defined by the suspension kinematic model presented in Subsection 2.2.2. In addition, the time derivative of $\boldsymbol{r}_{Vi,V}$, provided by Equation (2-50), results in

$$\dot{\boldsymbol{r}}_{Vi,V} = \frac{\partial \boldsymbol{r}_{Vi,V}}{\partial z_i}\dot{z}_i + \frac{\partial \boldsymbol{r}_{Vi,V}}{\partial u_*}\dot{u}_* = \boldsymbol{t}_{iz}\dot{z}_i + \boldsymbol{t}_{iu_*}\dot{u}_* \tag{2-58}$$

where $\boldsymbol{t}_{iz}$ and $\boldsymbol{t}_{iu_*}$ represents the partial velocities of the wheel-i relative to z_i and u_* respectively, and $u_* = u_F$ for $i = 1, 2$ (front rack displacement) and $u_* = u_R$ for $i = 3, 4$ (rear rack displacement). In addition, the wheel's orientation is defined by the knuckle's orientation because both of them are attached to the same reference frame W. Therefore, the angular velocity of the knuckle relative to the vehicle-fixed axis system V can be obtained as

$$\boldsymbol{\omega}_{0Ki,V} = \boldsymbol{\omega}_{0V,V} + \boldsymbol{\omega}_{Vi,V}, \tag{2-59}$$

and $\boldsymbol{\omega}_{Vi,V}$, similarly to the wheel's body position $\boldsymbol{r}_{Vi,V}$, can be expressed as follows

$$\boldsymbol{\omega}_{Vi,V} = \boldsymbol{d}_{iz}\dot{z}_i + \boldsymbol{d}_{iu*}\dot{u}_* \tag{2-60}$$

where $\boldsymbol{d}_{iz}$ and $\boldsymbol{d}_{iu*}$ are the partial angular velocities of the knuckle and u_* follows the same rule as presented before. Finally, the absolute angular velocity of the wheel-i is given by

$$\boldsymbol{\omega}_{0W_i,V} = \boldsymbol{\omega}_{0V,V} + \boldsymbol{\omega}_{Vi,V} + \boldsymbol{A}_{Vi}\boldsymbol{e}_{yR_i,i}\dot{\varphi}_i \tag{2-61}$$

where $\boldsymbol{A}_{Vi}\boldsymbol{e}_{yR_i,i}\dot{\varphi}_i$ describe the angular velocity due to the rotation speed of the wheel-i measured in the vehicle-fixed axis system V. Finally, velocities and angular velocities of all the bodies are summarized in Table 3.

Table 3: Velocities and angular velocities of all bodies relative to the vehicle-fixed axis system V.

Frame		Velocity	Angular velocity
V		$\boldsymbol{v}_{0V,V} = \boldsymbol{A}_{0V}^T \begin{bmatrix} \dot{x} \\ \dot{y} \\ \dot{z} \end{bmatrix}$	$\boldsymbol{\omega}_{0V,V} = \begin{bmatrix} 1 & 0 & -\sin\beta \\ 0 & \cos\alpha & \sin\alpha\cos\beta \\ 0 & -\sin\alpha & \cos\alpha\cos\beta \end{bmatrix} \begin{bmatrix} \dot{\alpha} \\ \dot{\beta} \\ \dot{\gamma} \end{bmatrix}$
i	K_i	$\boldsymbol{v}_{0V,V} + \boldsymbol{\omega}_{0V,V} \times \boldsymbol{r}_{Vi,V} + \boldsymbol{t}_{iz}\dot{z}_i + \boldsymbol{t}_{iu_*}\dot{u}_*$	$\boldsymbol{\omega}_{0V,V} + \boldsymbol{d}_{iz}\dot{z}_i + \boldsymbol{d}_{iu*}\dot{u}_*$
	W_i		$\boldsymbol{\omega}_{0V,V} + \boldsymbol{d}_{iz}\dot{z}_i + \boldsymbol{d}_{iu*}\dot{u}_* + \boldsymbol{A}_{Vi}\boldsymbol{e}_{yR_i,i}\dot{\varphi}_i$
C		$\boldsymbol{v}_{0V,V} + \boldsymbol{\omega}_{0V,V} \times \boldsymbol{r}_{VC,V}$	$\boldsymbol{\omega}_{0V,V}$

Accelerations

Chassis-fixed axis system C – The absolute acceleration of C can be calculated using the chassis velocity defined in Table 3 as follows

$$\boldsymbol{a}_{0C,V} = \frac{d}{dt}\boldsymbol{v}_{0C,V} = \dot{\boldsymbol{v}}_{0V,V} + \dot{\boldsymbol{\omega}}_{0V,V} \times \boldsymbol{r}_{VC,V} + \boldsymbol{\omega}_{0V,V} \times \boldsymbol{v}_{0C,V} \tag{2-62}$$

where $\boldsymbol{r}_{VC,V} = \text{const.}$ was considered. Then, the absolute angular acceleration

is obtained via

$$\boldsymbol{\alpha}_{0C,V} = \frac{d}{dt}\boldsymbol{\omega}_{0C,V} = \dot{\boldsymbol{\omega}}_{0V,V} + \boldsymbol{\omega}_{0V,V} \times \boldsymbol{\omega}_{0C,V} \tag{2-63}$$

where because $\boldsymbol{\omega}_{0C,V} = \boldsymbol{\omega}_{0V,V}$ their cross-product is equal to zero and therefore, $\boldsymbol{\alpha}_{0C,V} = \dot{\boldsymbol{\omega}}_{0V,V}$.

Wheel body-fixed axis system i – The acceleration of the wheel body-i relative to V can be calculated by the derivation of its velocity shown in Table 3 as follows

$$\begin{aligned} \boldsymbol{a}_{0i,V} = \frac{d}{dt}\boldsymbol{v}_{0i,V} &= \dot{\boldsymbol{v}}_{0V,V} + \dot{\boldsymbol{\omega}}_{0V,V} \times \boldsymbol{r}_{Vi,V} + \boldsymbol{t}_{iz}\ddot{z}_i + \boldsymbol{t}_{iu_*}\ddot{u}_* \\ &+ \boldsymbol{\omega}_{0V,V} \times \dot{\boldsymbol{r}}_{Vi,V} + \dot{\boldsymbol{t}}_{iz}\dot{z}_i + \dot{\boldsymbol{t}}_{iu_*}\dot{u}_* + \boldsymbol{\omega}_{0V,V} \times \boldsymbol{v}_{0i,V} \end{aligned} \tag{2-64}$$

Using the information of the angular velocities shown in Table 3, it is possible to express the absolute angular acceleration of the knuckle-i via

$$\begin{aligned} \boldsymbol{\alpha}_{0K_i,V} = \frac{d}{dt}\boldsymbol{\omega}_{0K_i,V} &= \dot{\boldsymbol{\omega}}_{0V,V} + \boldsymbol{d}_{iz}\ddot{z}_i + \boldsymbol{d}_{iu_*}\ddot{u}_* \\ &+ \dot{\boldsymbol{d}}_{iz}\dot{z}_i + \dot{\boldsymbol{d}}_{iu_*}\dot{u}_* + \boldsymbol{\omega}_{0V,V} \times \boldsymbol{\omega}_{0K_i,V} \end{aligned} \tag{2-65}$$

and the absolute angular acceleration of the wheel-i is given by

$$\begin{aligned} \boldsymbol{\alpha}_{0W_i,V} = \frac{d}{dt}\boldsymbol{\omega}_{0W_i,V} &= \dot{\boldsymbol{\omega}}_{0V,V} + \boldsymbol{d}_{iz}\ddot{z}_i + \boldsymbol{d}_{iu_*}\ddot{u}_* + \boldsymbol{A}_{Vi}\boldsymbol{e}_{yRi,i}\ddot{\varphi}_i \\ &+ \dot{\boldsymbol{d}}_{iz}\dot{z}_i + \dot{\boldsymbol{d}}_{iu_*}\dot{u}_* + \boldsymbol{\omega}_{Vi,V} \times \boldsymbol{A}_{Vi}\boldsymbol{e}_{yRi,i}\dot{\varphi}_i + \boldsymbol{\omega}_{0V,V} \times \boldsymbol{\omega}_{0W_i,V} \end{aligned} \tag{2-66}$$

2.2.5 Equations of motion

With the velocities and accelerations of all the bodies of the multibody vehicle model already defined then, it is necessary a method to derive the equations of motion of the system.

The Jourdain's principle

As written in [68], the Jourdain's principle (1908) states:

> *A constrained mechanical systems performs motions such that the total virtual power of the constraint forces and torques δP^c is zero.*

For a multibody system of $\boldsymbol{k}$ rigid bodies, the Jourdain's principle can be applied as follows

$$\delta P^c = \sum_{i=1}^{k} \left[\delta \boldsymbol{v}_i^T \boldsymbol{F}_i^c + \delta \boldsymbol{\omega}_i^T \boldsymbol{T}_i^c\right] = 0 \tag{2-67}$$

The virtual velocities δv_i and $\delta\omega_i$ are arbitrary and infinitesimal variations of the velocity and angular velocity of the body i. In addition, these virtual velocities are completely compatible with the constraint at any time and at any position, and are defined via

$$\delta \boldsymbol{v}_i = \frac{\partial \boldsymbol{v}_i}{\partial \boldsymbol{z}}\delta \boldsymbol{z} \quad \text{and} \quad \delta \boldsymbol{\omega}_i = \frac{\partial \boldsymbol{\omega}_i}{\partial \boldsymbol{z}}\delta \boldsymbol{z} \tag{2-68}$$

where $\boldsymbol{z}$ is a vector that collects the generalized speeds. Furthermore, the translational motion of a rigid body i is governed by Newton's law as

$$m_i \boldsymbol{a}_{0i} = \boldsymbol{F}_i^a + \boldsymbol{F}_i^c \tag{2-69}$$

and the rotational motion by Euler equation via

$$\boldsymbol{\Theta}_i \boldsymbol{\alpha}_{0i} + \boldsymbol{\omega}_{0i} \times \boldsymbol{\Theta}_i \boldsymbol{\omega}_{0i} = \boldsymbol{T}_i^a + \boldsymbol{T}_i^c \tag{2-70}$$

where the total force and torque were divided in the applied and constraint forces and torques respectively. Then, by employing equations (2-67), (2-68), (2-69) and (2-70), it is possible to obtain the equations of motion of the mechanical system as follows

$$\boldsymbol{K}(\boldsymbol{q})\,\dot{\boldsymbol{q}} = \boldsymbol{z}, \quad \boldsymbol{M}(\boldsymbol{q})\,\dot{\boldsymbol{z}} = \boldsymbol{g}(\boldsymbol{q}, \boldsymbol{z}) \tag{2-71}$$

where $\boldsymbol{M}(\boldsymbol{q})$ is know as the mass matrix and is given by

$$\boldsymbol{M}(\boldsymbol{q}) = \sum_{i=1}^{k} \left\{ \frac{\partial \boldsymbol{v}_{0i}^T}{\partial \boldsymbol{z}} m_i \frac{\partial \boldsymbol{v}_{0i}}{\partial \boldsymbol{z}} + \frac{\partial \boldsymbol{\omega}_{0i}^T}{\partial \boldsymbol{z}} \boldsymbol{\Theta}_i \frac{\partial \boldsymbol{\omega}_{0i}}{\partial \boldsymbol{z}} \right\} \tag{2-72}$$

and $\boldsymbol{g}(\boldsymbol{q}, \boldsymbol{z})$ is the vector of generalized forces and torques and is defined via

$$\boldsymbol{g}(\boldsymbol{q}, \boldsymbol{z}) = \sum_{i=1}^{k} \left\{ \frac{\partial \boldsymbol{v}_{0i}^T}{\partial \boldsymbol{z}} (\boldsymbol{F}_i^a - m_i \boldsymbol{a}_{0i}^R) + \frac{\partial \boldsymbol{\omega}_{0i}^T}{\partial \boldsymbol{z}} (\boldsymbol{T}_i^a - \boldsymbol{\Theta}_i \boldsymbol{\alpha}_{0i}^R - \boldsymbol{\omega}_{0i} \times \boldsymbol{\Theta}_i \boldsymbol{\omega}_{0i}) \right\} \tag{2-73}$$

and

$$\boldsymbol{q} = [x, y, z, \alpha, \beta, \gamma, z_1, z_2, u_F, z_3, z_4, u_R, \varphi_1, \varphi_2, \varphi_3, \varphi_4] \tag{2-74}$$

where $\boldsymbol{q}$ is a vector that collects the generalized coordinates of the vehicle, $\boldsymbol{K}$ is the kinematic matrix used to define an appropriate vector of generalized speeds $\boldsymbol{z}$, i.e.

$$\boldsymbol{z} = [v_{0V}^x, v_{0V}^y, v_{0V}^z, \omega_{0V}^x, \omega_{0V}^y, \omega_{0V}^z, \dot{z}_1, \dot{z}_2, \dot{u}_F, \dot{z}_3, \dot{z}_4, \dot{u}_R, \omega_1, \omega_2, \omega_3, \omega_4]. \tag{2-75}$$

where $[v_{0V}^x, v_{0V}^y, v_{0V}^z]$ and $[\omega_{0V}^x, \omega_{0V}^y, \omega_{0V}^z]$ are the components of $\boldsymbol{v}_{0V,V}$ and $\boldsymbol{\omega}_{0V,V}$, see Table 3, and $\omega_i = \dot{\varphi}_i$ is the spin speed of the wheel-i. Furthermore, the partial velocities $\frac{\partial \boldsymbol{v}_{0i}^T}{\partial \boldsymbol{z}}$ and partial angular velocities $\frac{\partial \boldsymbol{\omega}_{0i}^T}{\partial \boldsymbol{z}}$ can be calculated using information from Table 3 and the vector of generalized speeds defined in

Equation (2-75). These partial velocities are summarized in Table 4 and 5. In these tables, 0 have the corresponding dimensions for the respective calculation of the mass-matrix and vector of generalized forces and torques, e.g. a vector $0 = 0_{3\times1}$ or a matrix $0 = 0_{3\times3}$.

Table 4: Partial velocities.

Body	Partial velocities $\frac{\partial v_{0i,V}}{\partial z_k}$											
	Vehicle		Front axle			Rear axle			Wheels			
	$v_{0V,V} = [v_x\ v_y\ v_z]^T$	$\omega_{0V,V} = [\omega_x\ \omega_y\ \omega_z]^T$	$\dot{z}_1$	$\dot{z}_2$	$\dot{u}_F$	$\dot{z}_3$	$\dot{z}_4$	$\dot{u}_R$	ω_1	ω_2	ω_3	ω_4
Knuckle + wheel - 1	$I_{3\times3}$	$\widetilde{r}^T_{V1,V}$	t_{1z}	0	t_{1u}	0	0	0	0	0	0	0
Knuckle + wheel - 2	$I_{3\times3}$	$\widetilde{r}^T_{V2,V}$	0	t_{2z}	t_{2u}	0	0	0	0	0	0	0
Knuckle + wheel - 3	$I_{3\times3}$	$\widetilde{r}^T_{V3,V}$	0	0	0	t_{3z}	0	t_{3u}	0	0	0	0
Knuckle + wheel - 4	$I_{3\times3}$	$\widetilde{r}^T_{V4,V}$	0	0	0	0	t_{4z}	t_{4u}	0	0	0	0
Chassis	$I_{3\times3}$	$\widetilde{r}^T_{VC,V}$	0	0	0	0	0	0	0	0	0	0

Table 5: Partial angular velocities.

		Partial angular velocities $\frac{\partial \omega_{0i,V}}{\partial z_k}$										
		Vehicle		Front axle			Rear axle			Wheels			
Body		$v_{0V,V} = [v_x\ v_y\ v_z]^T$	$\omega_{0V,V} = [\omega_x\ \omega_y\ \omega_z]^T$	$\dot{z}_1$	$\dot{z}_2$	$\dot{u}_F$	$\dot{z}_3$	$\dot{z}_4$	$\dot{u}_R$	ω_1	ω_2	ω_3	ω_4
1	Knuckle	0	$I_{3\times3}$	d_{1z}	0	d_{1u}	0	0	0	0	0	0	0
	Wheel	0	$I_{3\times3}$	d_{1z}	0	d_{1u}	0	0	0	$e_{yR_1,V}$	0	0	0
2	Knuckle	0	$I_{3\times3}$	0	d_{2z}	d_{2u}	0	0	0	0	0	0	0
	Wheel	0	$I_{3\times3}$	0	d_{2z}	d_{2u}	0	0	0	0	$e_{yR_2,V}$	0	0
3	Knuckle	0	$I_{3\times3}$	0	0	0	d_{3z}	0	d_{3u}	0	0	0	0
	Wheel	0	$I_{3\times3}$	0	0	0	d_{3z}	0	d_{3u}	0	0	$e_{yR_3,V}$	0
4	Knuckle	0	$I_{3\times3}$	0	0	0	0	d_{4z}	d_{4u}	0	0	0	0
	Wheel	0	$I_{3\times3}$	0	0	0	0	d_{4z}	d_{4u}	0	0	0	$e_{yR_4,V}$
Chassis		0	$I_{3\times3}$	0	0	0	0	0	0	0	0	0	0